Applied Surface Science 347 (2015) 392–400

Contents lists available at ScienceDirect

Applied Surface Science

journal homepage: www.elsevier.com/locate/apsusc

Simultaneous removal of elemental mercury and NO from flue gas by V_2O_5–CeO_2/TiO_2 catalysts

Xunan Zhang[a,b], Caiting Li[a,b,*], Lingkui Zhao[a,b], Jie Zhang[a,b], Guangming Zeng[a,b], Yin'e Xie[a,b], Ming'e Yu[a,b]

[a] College of Environmental Science and Engineering, Hunan University, Changsha 410082, China
[b] Key Laboratory of Environmental Biology and Pollution Control (Hunan University), Ministry of Education, Changsha 410082, China

ARTICLE INFO

Article history:
Received 14 February 2015
Received in revised form 2 April 2015
Accepted 6 April 2015
Available online 14 April 2015

Keywords:
Elemental mercury
Selective catalytic reduction
Multi-pollutants control
Catalytic activity
V_2O_5–CeO_2/TiO_2

ABSTRACT

A series of Ce-doped V_2O_5/TiO_2 catalysts synthesized by an ultrasound assisted impregnation method were employed to investigate simultaneous removal of elemental mercury (Hg^0) and NO in lab-scale experiments. Scanning electron microscopy (SEM), Brunauer–Emmett–Teller (BET), X-ray diffractogram (XRD), and X-ray photoelectron spectroscopy (XPS) analyses were used to characterize the samples. Compared to TiO_2 support, the catalytic performance of CeO_2 doped on both TiO_2 and V_2O_5/TiO_2 catalysts have been improved. Remarkably, 1%V_2O_5–10% CeO_2/TiO_2 (V1Ce10Ti) exhibited the highest Hg^0 oxidation efficiency of 81.55% at 250 °C with a desired NO removal efficiency under the same condition. Both the NO conversion and Hg^0 oxidation efficiency were enhanced in the presence of O_2. The activity was inhibited by the injection of NH_3 with the increase of NH_3/NO. When in the presence of 400 ppm SO_2, Hg^0 oxidation was slightly affected. Furthermore, Hg^0 removal behavior under both oxidation and selective catalytic reduction (SCR) condition over V1Ce10Ti were well investigated to further probe into the feasibility of one single unit for multi-pollutants control in industry application. The existence of the redox cycle of $V^{4+} + Ce^{4+} \leftrightarrow V^{5+} + Ce^{3+}$ in V_2O_5–CeO_2/TiO_2 catalyst could not only greatly improve the NO conversion, but also promote the oxidation of Hg^0.

1. Introduction

Mercury has been listed as one of the most hazardous and toxic pollutants by the laws and regulations of more and more countries or regions due to its heavy metal characteristics, volatility, and bioaccumulation [1–3]. The Mercury Treaty that agreed by more than 140 nations during the Minamata convention on October 2013 was a great international effort to address global mercury emissions and releases. According to the reports, coal-fired utilities are currently the largest single anthropogenic emission source of mercury around the world, especially in the two giant economic entities China and the United States where power generation is largely dependent on coal consumption [4,5]. There are currently several technologies available to control mercury emissions, including activated carbon injection (ACI) capture, catalytic oxidation, photochemical oxidation, and existing air pollution control devices (APCDs) [2]. However, considering the obvious disadvantage such as high cost, narrow temperature range of application and slow regeneration rates, there is no wide application technology on mercury emission control yet [6]. Aimed at solving the problem that the ACI technology is costly and that the actual situation of China's coal-based energy structure will remaining inevitably in the next 50 years, catalytic oxidation of mercury by effective metal oxides catalysts, followed by the co-benefit capture of existing APCDs, such as fabric filters (FFs), electrostatic precipitators (ESPs), or wet flue gas desulfuration devices (WFGD) located in the power plants, is of high interests [7].

Among the three basic forms of mercury released from coal-fired flue gas, namely elemental mercury (Hg^0), oxidized mercury (Hg^{2+}), and particulate bound mercury (Hg_p), Hg^0 with high volatility and low solubility, is the dominant mercury species emitted to the atmosphere from the power plants for its persistence in the flue gas [8]. It has been observed that selective catalytic reduction (SCR) of nitrogen oxides (NOx, including NO, NO_2, and N_2O), which is widely used in stationary sources including coal-fired power plants due to its higher efficiency, selectivity and economic feasibility, could facilitate the catalytic oxidation of Hg^0 to Hg^{2+} in laboratory, bench scale and full-field tests [9–11]. The formed Hg^{2+} is highly

* Corresponding author at: College of Environmental Science and Engineering, Hunan University, Changsha 410082, China. Tel.: +86 731 88649216; fax: +86 731 88649216.
E-mail addresses: ctli@hnu.edu.cn, ctli3@yahoo.com (C. Li).

http://dx.doi.org/10.1016/j.apsusc.2015.04.039
0169-4332/

water-soluable and can be captured efficiently in WFGD systems. In particular, with vast SCR installation in coal-fired power plants and other flue combustion sites for NOx emission control, to make good use of SCR catalysts for Hg^0 conversion is worthy of being paid more attention, and in this way a novel economical process that has a remarkable efficiency on multi-pollutants control is finally expected.

Nitrogen oxides (NO, NO_2, and N_2O) emitted from automobiles and stationary sources are major causes of photochemical smog, acid rain, ozone depletion and greenhouse effects [12,13]. So far, the catalysts that most commercial used in the selective catalysis reduction (SCR) of NOx are mainly V_2O_5/TiO_2 based one, which could be promoted by other components, like WO_3 or MoO_3. Yu et al. [14] synthesized $V_2O_5–WO_3/TiO_2$ catalyst with different impregnation procedure and found that the wet impregnated catalyst shows higher SCR activities compared with the dry-impregnated one due to the different vanadia species generated on the surface of catalyst. It has been believed that high surface area titania has been recognized as the best carrier for this high-efficiency catalysts because it is only weakly and reversibly sulfated in the presence of SO_2 and oxygen, and makes catalysts more active than those obtained with other supports due to promoting effect. Many novel and effective metal oxides catalysts supported on TiO_2, such as $MnOx/TiO_2$ [15], CuO/TiO_2 [16], SiO_2/TiO_2 [17], CeO_2/TiO_2 [18,19], $CeO_2–WO_3/TiO_2$ [20], $MnOx/CeO_2–TiO_2$ [21,22], and $V_2O_5–WO_3–CeO_2/TiO_2$ [23], have been extensively investigated as potential SCR catalysts. Meanwhile, these promising catalysts have been also used to capture another important pollutant—mercury in the flue gas. Recently, the addition of ceria (CeO_2) have been drawn much attention on its potential use as a support, a promoter, or an active species [24]. In our previous works, cerium oxide was found to have superior activity and stability on Hg^0 capture when doped on various supports, including activated carbon[25], activated carbon fiber [26], activated coke[27], γ-Al_2O_3 [28], and HZSM-5 zeolite [29] due to its large oxygen storage capacity and unique redox couple Ce^{3+}/Ce^{4+}. It is believed that labile oxygen vacancies and bulk oxygen species with relatively high mobility are easily formed during the redox shift between Ce^{3+} and Ce^{4+} under oxidizing and reducing conditions, respectively. Li et al. [30] reported that CeO_2/TiO_2 catalayst with a weight ratio of 1–2 exhibited the highest Hg^0 catalytic oxidation activity with higher than 90% efficiency at 150–250 °C in simulated low rank (sub-bituminous and lignite) coal combustion flue gas. He et al. [31] introduced ceria to modify manganese oxide/titania materials for removal of mercury from flue gas, resulting in an excellent mercury capture capability in the presence of CO and NO at 175 °C. As mentioned above, CeO_2 could provide a promotional effect on both NO_x removal and mercury oxidation. Considering the important active role of V_2O_5 on NOx removal and its synergistic effect on TiO_2 support, a vanadium-based catalyst is ideal to be chosen as the reference. Liu et al. [32] investigated the effect of Ce on the activity and alkali resistance of V_2O_5/TiO_2 catalyst for SCR of NOx by NH_3 and found that the redox cycle ($V^{4+} + Ce^{4+} \leftrightarrow V^{5+} + Ce^{3+}$) can account for the excellent NH_3-SCR catalytic performance of $0.5\%V_2O_5–5\%CeO_2/TiO_2$ catalyst. However, neither the potential capability of the $V_2O_5–CeO_2/TiO_2$ catalyst on mercury removal nor the simultaneous removal of these two air pollutants has been studied yet before. To better understand the co-benefit of mercury removal by SCR catalysts utilized in most of coal-fired plants, it is of highly interest to study the removal of NOx and gaseous mercury simultaneously from the flue gas in one single unit.

In this study, $V_2O_5–CeO_2/TiO_2$ catalysts were developed and the relevant experiments on the activity of NO removal and Hg^0 oxidation were conducted. Besides, the effects of CeO_2 loading value, reaction temperature, and flue gas components including NH_3/NO, SO_2, O_2, were evaluated in a lab-scale reaction system. To further investigate the changes of physicochemical properties enhanced by the addition of CeO_2, scanning electron microscopy (SEM), Brunauer–Emmett–Teller (BET), X-ray diffractogram (XRD), and X-ray photoelectron spectroscopy (XPS) analyses were carried out and analyzed comprehensively. Given the sufficient and available experimental results and characteristics of the samples, the possible reaction mechanisms involved in the Hg^0 oxidation and NO conversion over $V_2O_5–CeO_2/TiO_2$ catalysts was proposed.

2. Experimental

2.1. Catalyst preparation

The anatase-type nanosize TiO_2 powder (Chengdu Ai Keda Chemical Technology Co.) was used as the carrier. *x*% CeO_2/TiO_2 (Ce*x*Ti, where Ce represents CeO_2, Ti represents TiO_2, and *x*, in the range of 0–15, represents the weight percentage of CeO_2, respectively) was prepared by wet impregnation method enhanced by ultrasound as follows: At first, a proper amount of cerium nitrate ($Ce(NO_3)_3{\cdot}6H_2O$) were dissolved into the deionized water to form the solution. Then TiO_2 powder was added to the solution. After stirring for 1 h, the mixture was exposed to an ultrasonic bath for 2 h, dried at 110 °C overnight and then calcined at 500 °C in static air for 4 h. Meanwhile, $1\%V_2O_5/TiO_2$ (noted as V1Ti) was prepared by the same method as described above using certain amount of ammonium metavanadate (NH_4VO_3) and oxalic acid solution instead. V1Ce*x*Ti catalyst was prepared by impregnating Ce*x*Ti powder with an oxalic acid solution of NH_4VO_3. After stirring for 1 h, the mixture was exposed to an ultrasonic bath for 2 h. The paste obtained was further dried at 110 °C overnight and then calcined at 500 °C in static air for 4 h. All the obtained samples were ground and sieved through 40–60 mesh.

2.2. Catalyst characterization

Brunauer–Emmett–Teller (BET) surface area analysis was performed by a Micromeritics Tristar II 3020 analyzer (Micromeritics Instrument Crop, USA). Prior to the BET measurements, all of the samples were oven dried at 110 °C overnight, and then degassed under vacuum at 180 °C for 12 h.

To further analyze the morphology and surface structure of the samples, scanning electron microscopy (SEM) photographs were obtained by means of the S-4800 analyzer (Hitachi Ltd. Japan) measurements analysis.

X-ray diffraction (XRD) measurements were carried out in a Rigaku rotaflex D/Max-C powder diffractometer (Rigaku, Japan) using nickel-filtered CuKa (k = 1.54 Å) radiation as an X-ray source to examine the crystallinity and dispersivity of each species on the support. The scanning range was 10° to 80° (2θ) with a step size of 0.02° and a step time of 2 min. The accelerating voltage and the applied current were 35 kV and 30 mA, respectively.

X-ray photoelectron spectroscopy (XPS) analysis was conducted at room temperature on a K-Alpha 1063 X-ray photoelectron spectrometer (Thermo Fisher Scientific, UK) with an Al K_a X-ray source. The observed spectra were calibrated with the C 1s binding energy (BE) value of 284.6 eV.

2.3. Experimental setup and procedure

The experimental apparatus for evaluating Hg^0 oxidation and NOx removal activities of the catalysts is shown in Fig. 1. The fixed bed reactor consisted of a digital temperature controller and a quartz tube with an inner diameter of 20 mm and a length of 60 cm. The digital temperature controller was employed to keep the fixed-bed reactor at desired temperature. All individual flue

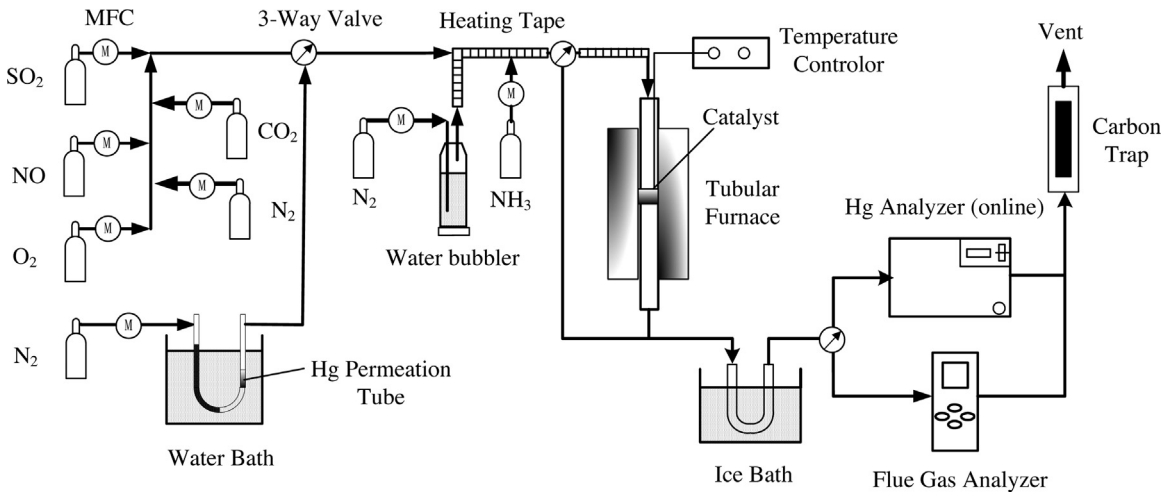

Fig. 1. Schematic diagram of the experimental setup.

gas components were from cylinder gases and were precisely controlled by mass flow controllers (MFC). The simulated composition of basic flue gas included 5% O_2 (99.999%), 500 ppm NO (20.0% NO + 80.0% N_2), 500 ppm NH_3 (99.999%), 400–1200 ppm SO_2 (20.4% SO_2 + 79.6% N_2, when used), 8% (vol) water vapor (when used) and N_2 (99.999%) as balance. The peristaltic pump transferred water into the stainless steel tube wrapped with a heating line and then H_2O (g) was generated. The Hg^0 vapor was generated by the U-shape device which was composed of an elemental mercury permeation tube (VICI Metronics Co., USA) and a water bath. One N_2 flow (150 mL/min) passed through the Hg^0 permeation tube and introduced the saturated Hg^0 vapor into the system with a desired water bath temperature. The Hg^0 concentration in the reactant gases was maintained at about 60 $\mu g/m^3$ for all the follow experiments. The total flow rate was maintained at 650 mL/min, corresponding to a gas hourly space velocity (GHSV) of 65,000 h^{-1}. A flue gas analyzer (Kane 950, UK) was used to measure the NO concentration while mercury concentration was online monitored by a RA-915-M Mercury Analyzer (Lumex Ltd., Russia; detection limit = 2 ng/m^3). After the analyses, the exhaust gas was firstly introduced into the activated carbon trap before being expelled into the atmosphere.

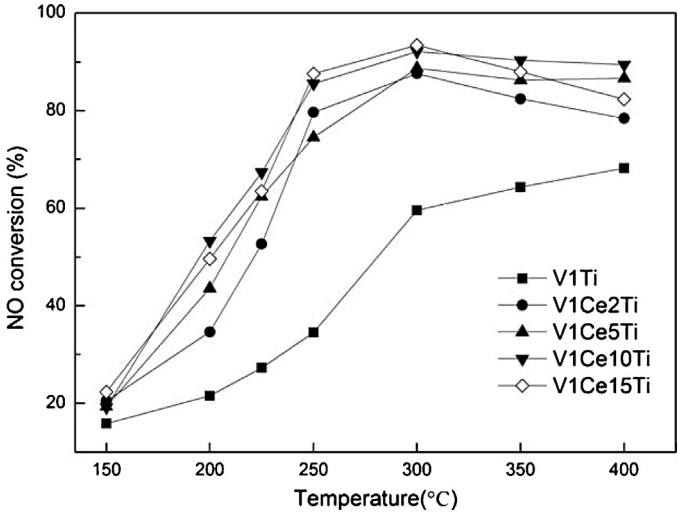

Fig. 2. NO conversion efficiency as a function of reaction temperature over V1CexTi catalysts. Reaction conditions: [NO] = [NH_3] = 500 ppm, [O_2] = 5 vol%, N_2 as balance, GHSV = 65,000 h^{-1}.

In each test, 0.5 g (about 0.6 mL) sample was packed in the quartz tube. The catalytic activities of NO conversion and Hg^0 oxidation were tested at 150–400 °C in the fixed bed reactor under atmospheric pressure. Two or more hours were maintained for each experiment set. At the beginning of each test, the gas stream bypassed the reactor bed and the inlet gas was sampled to ensure a stable NO and Hg^0 feed concentration. Then, the gas flow was switched to pass through the catalysts and the gas compositions in the outlet were measured. For the whole test, the loss of Hg^0 over the catalysts should be due to the oxidation or adsorption of Hg^0. Nevertheless, it is generally agreed that most of the release of Hg^0 concentration across the catalysts is attributed to Hg^0 oxidation and the major speciation of mercury is identified as the oxidized mercury (Hg^{2+}). Hg^0 oxidation efficiency ($\eta_{Hg\text{-}oxi}$) over the catalysts was calculated by Eq. (1). A mercury speciation conversion system was used to measure the surface deposit of mercury in our previous study. The results showed that total elemental mercury (Hg^T) removal efficiency (quantified by the Eq. (2) and noted as $\eta_{Hg\text{-}cap}$) was slightly larger than Hg^0 oxidation efficiency ($\eta_{Hg\text{-}oxi}$) in this study. Therefore, the Hg^0 removal efficiency (E_{oxi}) is calculated by the Eq. (1).

$$\eta_{Hg\text{-}oxi}(\%) = \frac{Hg^0_{in} - Hg^0_{out}}{Hg^0_{in}} \times 100\% \quad (1)$$

$$\eta_{Hg\text{-}cap}(\%) = \frac{Hg^0_{in} - Hg^0_{out}}{Hg^0_{in}} \times 100\% \quad (2)$$

where $Hg^0{}_{in}$ and $Hg^0{}_{out}$ are the concentrations of Hg^0 ($\mu g/m^3$) at the inlet and outlet of reactor, respectively.

Meanwhile, NO is mainly reduced to N_2 in SCR of NOx reaction, formation of other N-containing products is ignored (e.g., N_2O and NO_2), allowing the NO conversion efficiency (η_{NO}) to be calculated using Eq. (3):

$$\eta_{NO}(\%) = \frac{NO_{in} - NO_{out}}{NO_{in}} \times 100\% \quad (3)$$

where NO_{in} and NO_{out} are the concentrations of NO (ppm) at the inlet and outlet of reactor, respectively.

Specifically, prior to testing the catalyst for Hg^0 capture, blank experiments were performed before the activity test to eliminate any possible interference from the reactor and flue gas components. The results showed negligible difference between the inlet and outlet data, which proved the inertness of the reactor system. Furthermore, the experimental errors in the experiments are

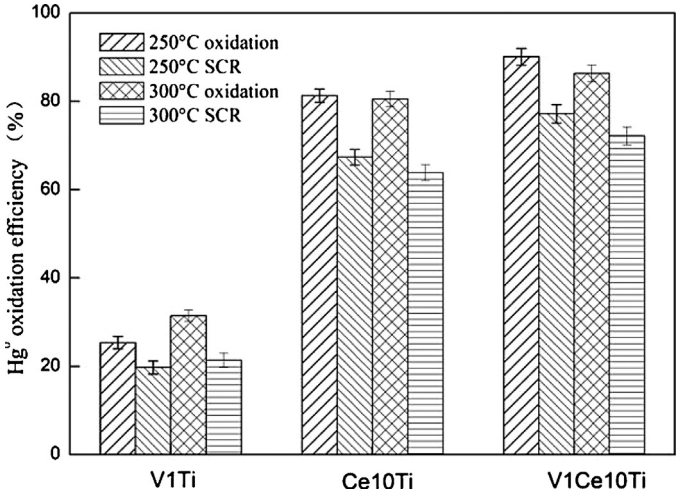

Fig. 3. Comparison of Hg^0 oxidation efficiency over V1Ti, Ce10Ti, and V1Ce10Ti under oxidation or SCR condition at 250–300 °C. Reaction conditions: $[O_2]$ = 5 vol%, $[N_2]$ as balance, GHSV = 65,000 h^{-1}, [NO] = $[NH_3]$ = 500 ppm (under SCR condition).

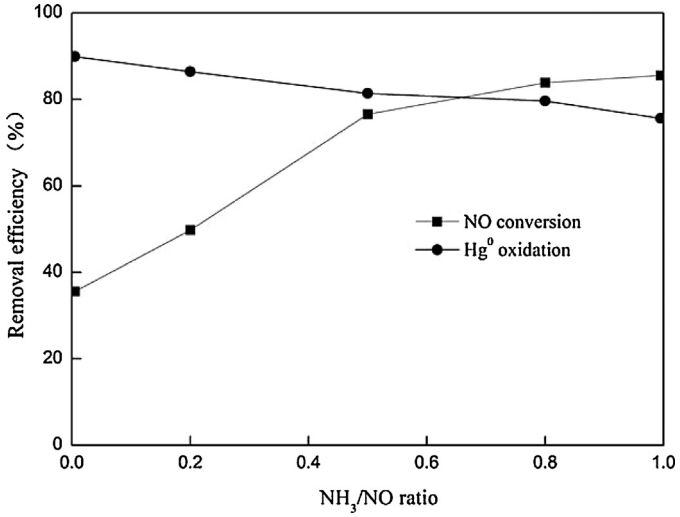

Fig. 4. Effect of NH_3/NO ratio on NO conversion and Hg^0 oxidation efficiency at 250 °C. Reaction conditions: $[O_2]$ = 5 vol%, $[NH_3]/[NO]$ = 0–1.0, $[N_2]$ as balance, GHSV = 65,000 h^{-1}.

inevitable. Hence, both the $\eta_{Hg\text{-}oxi}$ and η_{NO} are the average of three or more replicates under similar experimental condition.

3. Results and discussion

3.1. Performance of catalysts

3.1.1. SCR catalytic activity

The SCR of NO with NH_3 over V1Ce*x*Ti catalysts with different ceria loading was carried out on the fix bed reaction system at 150–400 °C under atmospheric pressure. The results were shown in Fig. 2. Considering the toxicity of vanadium to the human body, a typical amount of 1% vanadium was employed in our experiments. V1Ce10Ti showed much higher catalytic activity than V1Ce2Ti, V1Ce5Ti, V1Ce15Ti, and TiO_2 support, especially at 250–300 °C. 91.25% NO conversion was achieved over V1Ce10Ti at 300 °C. It is obvious that the addition of 10% CeO_2 significantly enhanced the NO conversion. There are several reasons for this promotional effect: For one, cubic CeO_2 pattern was identified after doping ceria on the titania in XRD analysis. The chemical reactions in the $Ti_xCe_{1-x}O_2$ complex oxides could increase the specific surface area and enhance the unique redox properties [33,34]. More importantly, it has been considered that the interaction between V and Ce could cause a distinct synergetic catalysis effect on the SCR of NO, which facilitates the NO conversion. The catalytic activity was also improved dramatically with the reaction temperature increasing from 150 °C to 300 °C, while slightly decreased with higher temperature. The range of 250–300 °C was the best reaction temperature for the SCR of NO with NH_3 over V1Ce*x*Ti catalysts.

3.1.2. Hg^0 oxidation catalytic activity

Many researches have recently reported that SCR catalysts could exhibit the co-benefit of promoting Hg^0 oxidation and capture in the flue gas in addition to NO_x removal [11,35,36]. To look into the potential of using as a multi-pollutants removal catalyst, V1Ce*x*Ti was also used to further investigate the capacity of Hg removal in the subsequent study. From the above NH_3-SCR activity test results, we chose the V1Ce10Ti as a potential Hg^0 capture material with its significant NO conversion activity. Meanwhile, Ce10Ti and V1Ti were used as the reference to get a better understanding of the role of Ce and V as active components.

Fig. 3 showed the results of Hg^0 oxidation efficiency over V1Ti, Ce10Ti, and V1Ce10Ti under both oxidation and SCR condition at 250–300 °C. A gas mixture containing 5% oxygen in N_2 balance was fed to the reactor system through mass flow controller under oxidation condition experiment. Under SCR condition experiment, NO and NH_3 of 500 ppm, respectively, were additionally fed to the compositions of oxidation condition. It can be seen that ceria greatly promoted the Hg^0 oxidation efficiency of V1Ti with a larger than 50% increase. V1Ce10Ti showed the best performance under oxidation condition at 250 °C. Specially, when feeding the NH_3 and NO into the flow gas, the Hg^0 oxidation efficiency decreased to some extent. The possible reason was that the reactive intermediates in the NH_3-SCR process, such as NH_4^+, NO_2 and monodentate nitrate species could inhibit the Hg^0 oxidation reaction on the surface of catalyst. Li et al. [37] observed that NO covered the active sites of catalyst and consumed surface oxygen active for Hg^0 oxidation, hence limiting Hg^0 oxidation. In some cases, NH_3 was found to be competing with the absorbed Hg^0, resulting in an inhibiting effect on Hg^0 oxidation.

3.2. Effect of individual flue gas components

3.2.1. Effect of NH_3/NO ratio

Since NH_3 was one of the indispensable reductant of NH_3-SCR of NO reaction, it is very important to identify the effect of NH_3 on the oxidation of Hg^0. Both the NO conversion and Hg^0 oxidation efficiency were examined with the change of NH_3/NO ratio. As shown in Fig. 4, with the increase of NH_3/NO, meaning more addition of NH_3, NO conversion was dramatically promoted in the NH_3-SCR reaction, while Hg^0 oxidation decreased conversely. Remarkably, 86.03% NO conversion and 77.64% Hg^0 oxidation efficiency was obtained over V1Ce10Ti when the NH_3/NO ratio was 1.0. As mentioned above, the condition of existing NH_3-SCR system was quite of paradoxical regarding to the NO conversion and Hg^0 oxidation. However, the obvious inhibiting effect of NH_3 might be reduced by the equimolar ratio between NH_3 and NO, or the on-going modifying of the catalysts.

3.2.2. Effect of O_2

Many researchers have reported that Cl- or O-species play the major role in affecting Hg^0 oxidation [27,38]. Meanwhile, O-species is considered to be important in the SCR catalysts, especially in the metal oxides catalysts. In this work, we investigated the effect of O_2 on activity of V1Ce10Ti. As is shown in Fig. 5, in the pure N_2 atmosphere, the NO conversion and Hg^0 oxidation efficiency were

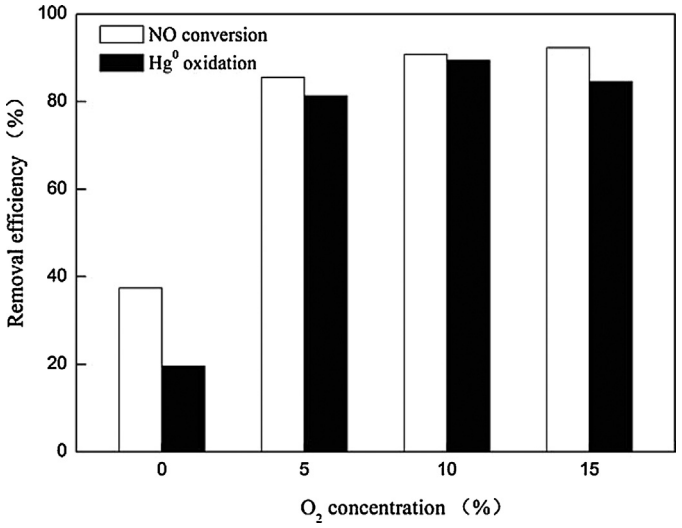

Fig. 5. Effect of O_2 concentration on NO conversion and Hg^0 oxidation efficiency over V1Ce10Ti at 250 °C. Reaction conditions: $[O_2]$ = 0 vol%, 5 vol%, 10 vol%, 15 vol%, $[NO] = [NH_3]$ = 500 ppm, $[N_2]$ as balance, GHSV = 65,000 h^{-1}.

less than 40% and 20%, respectively. When the O_2 concentration increased from 2% to 15%, the activity of V1Ce10Ti was significantly enhanced. It indicated that O_2 could be beneficial to the catalyst's capability. As the XPS analysis proved, it was possible that gas-phase O_2 regenerated the lattice oxygen and replenished the chemisorbed oxygen, which facilitated Hg^0 oxidation. And HgO might be the main oxidized mercury that accumulated on catalyst surface [39].

3.2.3. Effect of SO_2

In the coal-derived flue gases, SO_2 is believed to be one of main components in the flue gas. The sulfur-tolerance of catalyst is necessary to be investigated. Fig. 6 showed the effect of SO_2 on the activity of V1Ce10Ti. It can be obviously seen in Fig. 6(a) that the activity of V1Ce10Ti was inhibited dramatically with the increase of SO_2 concentration at 250 °C. When 1200 ppm SO_2 was added in the flow gas, about 25.5% of NO conversion efficiency and 38.7% of Hg^0 oxidation efficiency was reduced, respectively. The deactivation of catalyst by SO_2 could be due to the reasons as follows: on one hand, the interaction between SO_2 and NH_3 in the flue gas leaded to the formation of ammonia sulfate on catalyst surface, thus inhibiting the NO conversion. On the other hand, SO_2 competed with Hg^0 for active sites, in which way it could deactivate the catalyst's capability in oxidizing Hg^0. Fig. 6(b) illustrated the SO_2 tolerance vs time on the activity of V1Ce10Ti. As is shown, when adding 400 ppm SO_2 into the stream, the NO conversion and Hg^0 oxidation efficiency decreased as observed above. After that, the SO_2 stream was cut off. It was found that the catalyst's capability was recovered gradually but not returned to the original level yet. Conclusively, the deactivation by SO_2 was irreversible somehow.

3.2.4. Effect of H_2O

To investigate the water-resistance of the catalyst, 8% water vapor was added into simulated flue gas quantificationally and continuously. As shown in Fig. 7, when 8% H_2O was added into the flue gas, both the NO conversion and Hg^0 oxidation efficiencies declined quickly, with an approximately 33% and 21% decrease respectively, and reached stable value after some times. When H_2O was cut off from the flue gas, the removal efficiencies of NO and Hg0 could restore to the some level but less than the original value. The inhibition of H_2O might be explained mainly by the strongly

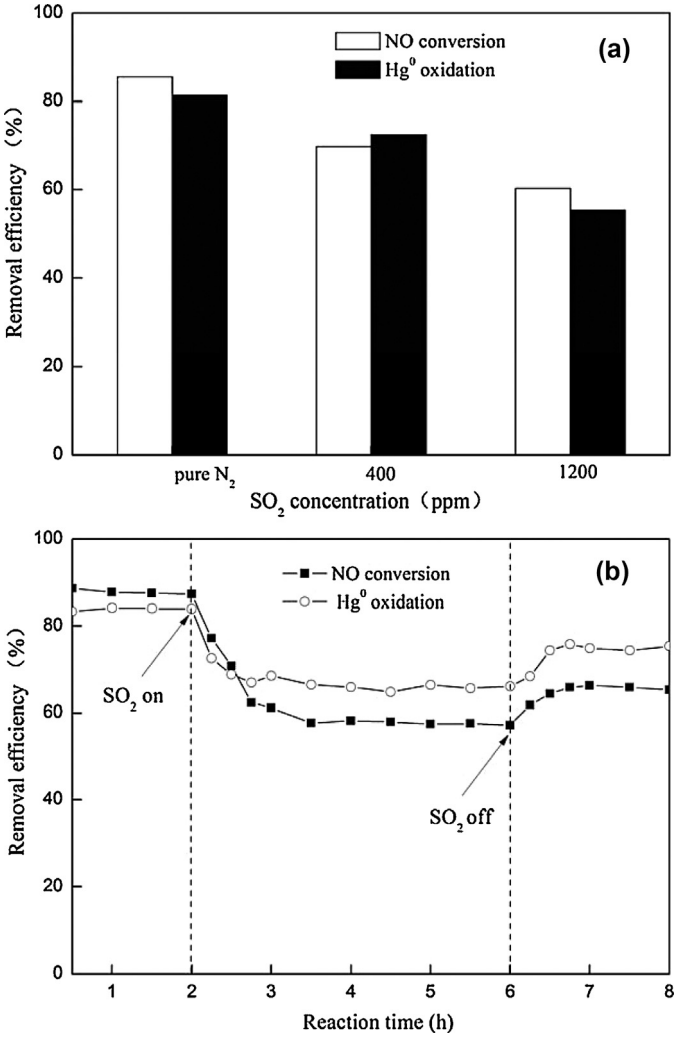

Fig. 6. Effect of SO_2 on NO conversion and Hg^0 oxidation efficiency over V1Ce10Ti at 250 °C in the flue gas of (a) 0–1200 ppm SO_2; (b) with or without 400 ppm SO_2; reaction conditions: $[O_2]$ = 5 vol%, $[NO] = [NH_3]$ = 500 ppm (under SCR condition), $[N_2]$ as balance, GHSV = 65,000 h^{-1}.

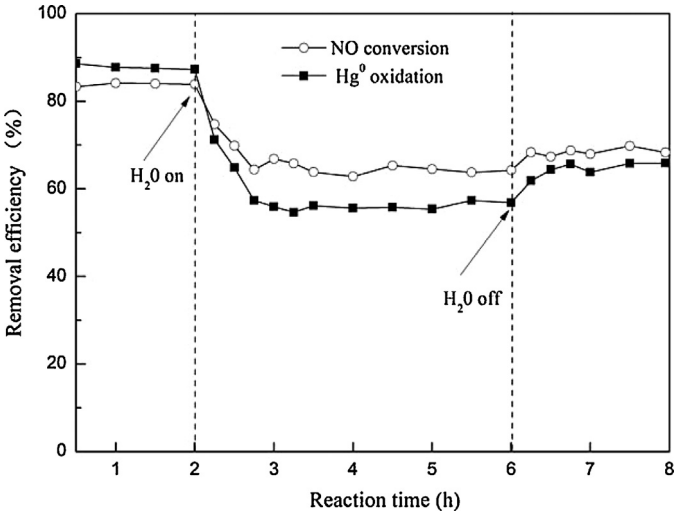

Fig. 7. Effect of H_2O on NO conversion and Hg^0 oxidation efficiency over V1Ce10Ti at 250 °C. Reaction conditions: $[H_2O]$ = 8 vol%, $[NO] = [NH_3]$ = 500 ppm, $[N_2]$ as balance, GHSV = 65,000 h^{-1}.

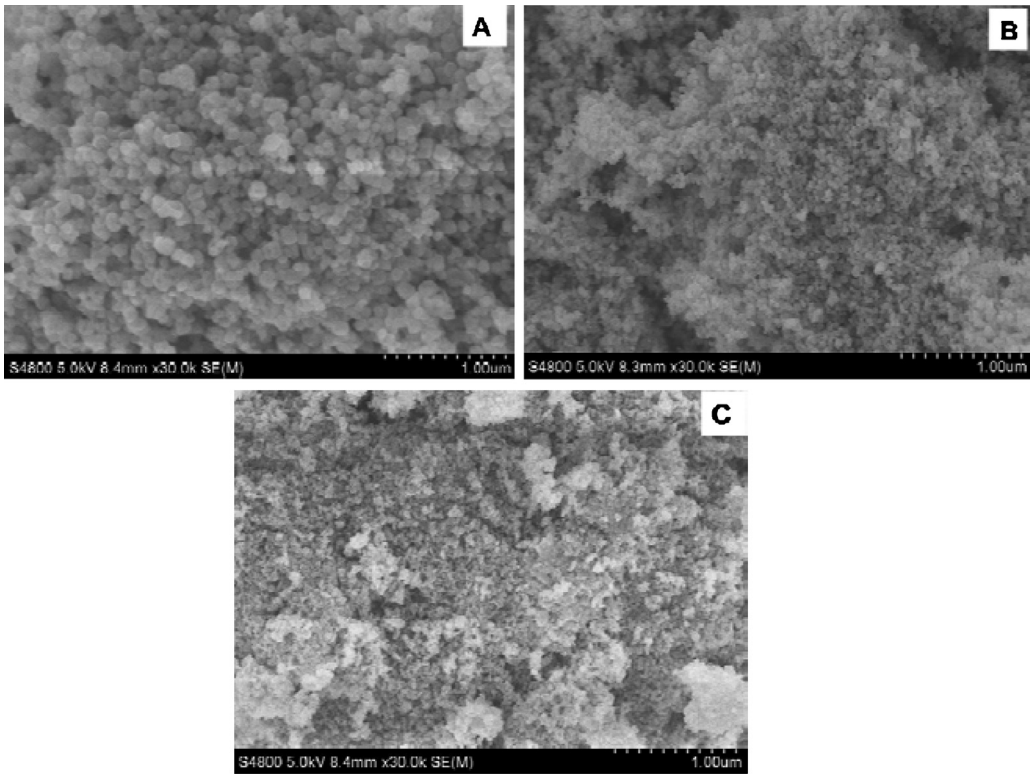

Fig. 8. SEM photographs of (A) pure TiO_2, (B) Ce10Ti, and (C) V1Ce10Ti.

Table 1
BET surface and pore parameters of the different catalysts.

Catalyst	BET surface area (m^2/g)	Pore volume (cm^3/g)	Average pore size (nm)
Pure TiO_2	57.58	0.172	11.366
V1Ti	44.79	0.186	15.546
Ce10Ti	72.42	0.156	8.823
V1Ce10Ti	68.64	0.163	9.284

competitive adsorption between active sites of the catalyst and Hg^0 or NO [17,40].

3.3. Characteristics of catalysts

3.3.1. BET analysis

The physical properties of V1Ti, Ce10Ti, and V1Ce10Ti catalysts including BET surface area (S_{BET}), total pore volume and average pore size were summarized in Table 1. It could be seen that the anatase-type nanosize TiO_2 support had a large S_{BET} of 57.58 m^2/g. V1Ce10Ti exhibited a larger S_{BET} than that of V1Ti and pure TiO_2, otherwise it was smaller than Ce10Ti. Comparatively, the average pore diameter decreased when doping V and Ce on TiO_2 support. The reasons for this result could be as follows: the typical anatase-type nanosize TiO_2, the support that used in our work, possessed desire surface area for the doping of CeO_2 and V_2O_5, which provided a well dispersion of the active component. Fang et al. [41] reported that TiO_2 and CeO_2 were in the anatase phase and the cubic fluorite phase in CeO_2–TiO_2 mixed oxides, respectively. And CeO_2–TiO_2 mixed oxides exhibited much higher surface areas than the individual oxides due to the formation of a Ce–O–Ti interface within TiO_2 anatase. Moreover, it has been reported that CeO_2 or other cerium compounds, which existed over the external surface of the catalysts, could interaction with vanadium compounds, in which way complex oxides like $CeVO_4$ might be formed [32,42].

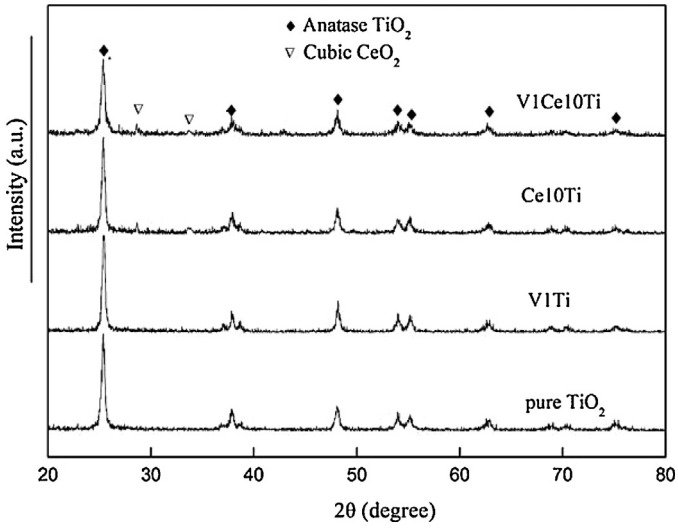

Fig. 9. XRD patterns of pure TiO_2, V1Ti, Ce10Ti, and V1Ce10Ti.

3.3.2. SEM analysis

Fig. 8 showed the SEM micrographs of pure TiO_2, Ce10Ti and the selected V1Ce10Ti samples. The characteristics of the anatase-type nanosize TiO_2 surface have changed according to various active components loading. It was observed that the crystallographic form of the pure TiO_2 was relatively distinct, while the crystallographic form of the CeO_2 was vague. It indicated that the cerium compounds could well dispersed on the TiO_2 and the good dispersion of CeO_2

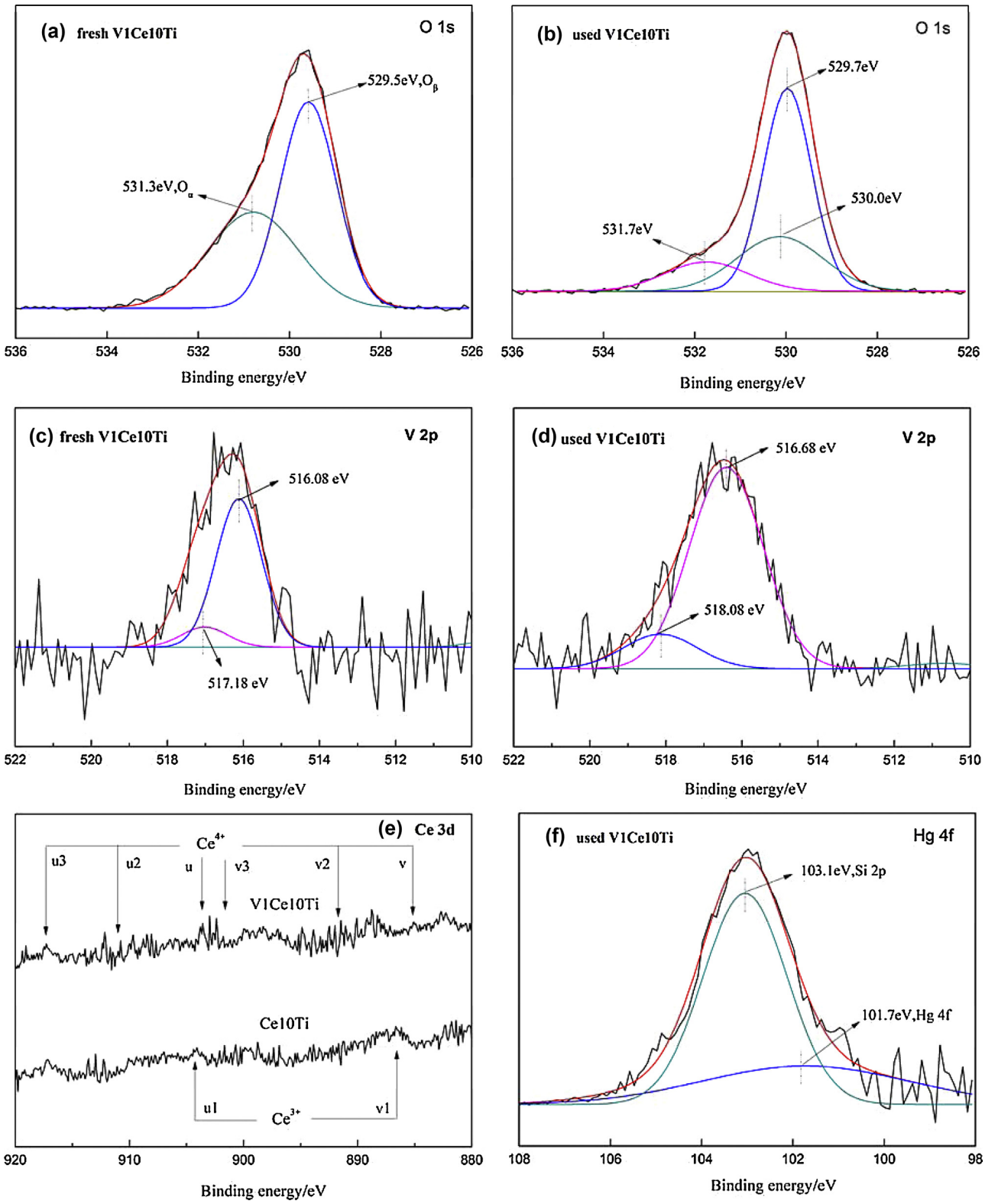

Fig. 10. (a) O1s XPS spectra of fresh V1Ce10Ti; (b) O1s XPS spectra of the used V1Ce10Ti; (c) V 2p XPS spectra of fresh V1Ce10Ti; (d) V 2p XPS spectra of the used V1Ce10Ti catalyst; (e) Ce 3d XPS spectra of Ce10Ti and V1Ce10Ti; (f) Hg 4f XPS spectra of the used V1Ce10Ti catalyst.

both on TiO_2 and V1Ti could account for the higher catalytic activity of the V1Ce*x*Ti catalyst in our experiments.

3.3.3. XRD analysis

The powder X-ray diffraction patterns of V1CexTi with different loading were shown in Fig. 9. Crystalline phases were identified by being compared with ICDD files. For all the pure TiO_2 support and TiO_2-supported catalysts, the anatase phase was the main phase. The anatase TiO_2 is recognized as desirable support for the NH_3-SCR catalyst as reported in many literature. The cubic crystalline phase of CeO_2 (PDF-#43-1002) was clearly detected (2θ = 28.62 and 35.16) both in Ce10Ti and V1Ce10Ti. Merely none of XRD patterns for crystalline V_2O_5 or other vanadium species such as $CeVO_4$ was observed, indicating that V species were highly dispersed on TiO_2 support. It was likely in the form of "monolayer" species at the surface of the TiO_2-anatase carrier, and these"monolayer" species were unable to be detected.

3.3.4. XPS analysis

Fig. 10(a) O1s XPS spectra of fresh V1Ce10Ti; (b) O1s XPS spectra of the used V1Ce10Ti; (c) V 2p XPS spectra of fresh V1Ce10Ti; (d) V 2p XPS spectra of the used V1Ce10Ti catalyst; (e) Ce 3d XPS spectra of Ce10Ti and V1Ce10Ti; (f) Hg 4f XPS spectra of the used V1Ce10Ti catalyst.

The XPS spectra of O 1s for the fresh and used V1Ce10Ti were presented in Fig. 10. There were two overlapping peaks observed in the fresh V1Ce10Ti, while three ones in the used V1Ce10Ti. The peaks could be fitted into two different oxygen species. One is the chemical oxygen with a binding energy of around 531.3–531.7 eV (denoted as O_α), the other is the lattice oxygen with a binding energy range of around 529.5–530.0 eV (denoted as O_β) [43]. It was worth noting that the used V1Ce10Ti (shown in Fig. 10(b)) possessed more O_α than that of fresh one, with the O_α/O_β ratio increasing from 1.34 to 1.62, meaning more O_β was consumed during the reaction. According to previous works, O_β might be easily bonded with adsorbed mercury to form HgO in the adsorption and oxidation reaction of Hg^0 over the surface of catalyst.

Fig. 10(c) and (d) showed the V 2p XPS spectra of fresh V1Ce10Ti and used one, respectively. Compared with the vanadium peak in the Fig. 10(c), the two V 2p XPS spectra peaks of the used V1Ce10Ti catalysts moved slightly towards to the binding energy (517.18 eV and 518.08 eV) of V^{5+} 2p 3/2 species. It could be implied that the V^{4+} was readily consumed to form a V^{4+}/V^{5+} redox couple on the surface of catalyst, which was not only a benefit for the NH_3-SCR reaction but a promotion for the mercury oxidation process. Besides, it has been reported that Hg^0 in flue gas can have a chemisorption reaction with V_2O_5 on catalyst surface and then can form V^{4+} intermediate products [44]. Yan et al. [40] employed various catalysts supported on titanium for Hg^0 conversion, and pointed that V_2O_5 was considered to be the main active component to Hg^0 conversion in SCR catalyst.

The XPS spectra of Ce 3d for Ce-doped catalysts were presented in Fig. 10(e). In accordance with previous studies [45], the spectrum of Ce 3d could be decomposed into eight components. The ones denoted as u are due to 3d 3/2 spin-orbit states and those denoted as v are the corresponding 3d 5/2 states. The six sub-bands labeled v, v2, v3, u, u2 and u3, are attributed to Ce^{4+}, otherwise the v1 and u1 ones represent the Ce^{3+} [27,46]. In comparison with Ce10Ti, there was much more appearance of Ce^{4+} on V1Ce10Ti with a remarkable increase of Ce^{4+}/Ce^{3+} ratio. Interestingly, we found that both the activity of NH_3-SCR of NO and Hg^0 oxidation over V1Ce10Ti was much higher than that of Ce10Ti, implying that the Ce^{4+} oxide played an important role in improving the performance of the catalyst.

To elucidate the transformation and capture behavior of Hg^0 over the surface of the catalyst, the XPS spectrum of Hg 4f was conducted and the result was shown in Fig. 10(f). As is shown, there were two peaks observed. The strong peak at 103.1 eV was ascribed to the Si 2p electron. And the other weak one with a binding energy of 101.7 eV was corresponding to Hg 4f. Hence, the binding energy of this Hg 4f peak was significantly higher than the 99.9 eV reference point for Hg^0 [47]. It can be attributed to HgO, which is in accordance with some previous observations by other authors [48]. And O species on the surface of catalyst was found to be beneficial to the Hg^0 oxidation accordingly.

3.4. Mechanism of Hg^0 and NO removal over V_2O_5–CeO_2/TiO_2

In this work, it was worthy noted that the reaction on the surface of CeO_2–V_2O_5/TiO_2 catalyst included both NO conversion and Hg^0 oxidation. Eventually a redox system was formed. NO was reduced by NH_3 through the catalysis of NH_3-SCR while Hg^0 was oxidized to Hg^{2+} species. The redox process is the major part in NH_3-SCR of NO, especially the synergetic effect between V and Ce. On one hand, the cerium in ceria can easily occupy two oxidation states [CeO_2 (Ce^{4+}) ↔ Ce_2O_3 (Ce^{3+})], thus allowing ceria to accommodate surface oxygen species (lattice oxygen, O_β). On the other hand, the vanadium is predominant part for the SCR reaction to proceed with the redox couples of V^{4+}/V^{5+}. Thus, in the surface of V_2O_5–CeO_2/TiO_2, the existence of the redox cycle of $V^{4+} + Ce^{4+} \leftrightarrow V^{5+} + Ce^{3+}$ (illuminated by Eq. (4)) could greatly improve the NO conversion. Moreover, the addition of Ce to TiO_2 contributes to the formation of monodenate nitrate and NO_2, which is beneficial to the Hg^0 oxidation [32].

Mars–Maessen mechanism proposed by Granite et al. [49] has been used to explain many reactions on the metal oxides catalysts. The detailed steps involved in Hg^0 oxidation could be as follows: Firstly, gaseous Hg^0 was adsorbed on the surface of catalyst by the physisorption to form Hg^0 (ad); then Hg^0 (ad) would be bonded with lattice oxygen and/or chemisorbed oxygen of the catalyst surface to form weakly bonded speciation Hg–M–O_{x-1} (M = V or/and Ce) and then formed mercuric oxide (HgO). It has been observed that the consumed lattice oxygen and/or surface oxygen can be replenished by the gas-phase O_2. The pathway could be explained by Eq. (5)–(8).

$$2VO_2 + 2CeO_2 \rightarrow V_2O_5 + Ce_2O_3 \quad (4)$$

$$Hg^0(g) \rightarrow Hg^0(ad) \quad (5)$$

$$Hg(ad) + O \rightarrow HgO \quad (6)$$

$$2CeO_2 \leftrightarrow Ce_2O_3 + O_\beta \quad (7)$$

$$O_\beta \leftrightarrow O \quad (8)$$

4. Conclusions

Considering the application in industry, especially in coal-fired plants in China, SCR catalyst has been considered a key role with the increasing installation in coal-fired plants in the last decades. In the present paper, Both NH_3-SCR of NO and Hg^0 oxidation behavior over V_2O_5–CeO_2/TiO_2 catalyst has been studied. V1Ce10Ti exhibited the highest Hg^0 oxidation efficiency of 81.55% at 250 °C with a desired NO removal efficiency under the same condition. The efficiency of Hg^0 oxidation under oxidation condition is better than that SCR condition, which was mainly attributed to the inhibiting effect of NH_3. O_2 could be a promoter for the catalyst's activity, while the addition of SO_2 played an irreversible inhibiting role on both NO and Hg^0 removal. The existence of the redox cycle of $V^{4+} + Ce^{4+} \leftrightarrow V^{5+} + Ce^{3+}$ in V_2O_5–CeO_2/TiO_2 catalyst could not only greatly improve the NO conversion, but also promote the oxidation of Hg^0. Consequently, we proposed one single step process for simultaneous removal of Hg^0 and NO from the flue gas.

Acknowledgement

This work was supported by the National High Technology Research and Development Program of China (863 Program) (2011AA060803) and the National Natural Science Foundation of China (51278177, 51478173).

References

[1] R.D. Vidic, D.P. Siler, Vapor-phase elemental mercury adsorption by activated carbon impregnated with chloride and chelating agents, Carbon 39 (2001) 3–14.
[2] R.K. Srivastava, N. Hutson, B. Martin, F. Princiotta, J. Staudt, Control of mercury emissions from coal-fired electric utility boilers, Environ. Sci. Technol. 40 (2006) 1385–1393.
[3] R. Stolle, H. Koeser, H. Gutberlet, Oxidation and reduction of mercury by SCR DeNOx catalysts under flue gas conditions in coal fired power plants, Appl. Catal. B: Environ. 144 (2014) 486–497.
[4] Q.C. Wang, W.G. Shen, Z.W. Ma, Estimation of mercury emission from coal combustion in China, Environ. Sci. Technol. 34 (2000) 2711–2713.
[5] A.P. Jones, J.W. Hoffmann, D.N. Smith, T.J. Feeley 3rd, J.T. Murphy, DOE/NETL's phase II mercury control technology field testing program: preliminary economic analysis of activated carbon injection, Environ. Sci. Technol. 41 (2007) 1365–1371.
[6] S. Sjostrom, M. Durham, C.J. Bustard, C. Martin, Activated carbon injection for mercury control: overview, Fuel 89 (2010) 1320–1322.
[7] H.Z. Tian, Y. Wang, K. Cheng, Y.P. Qu, J.M. Hao, Z.G. Xue, F.H. Chai, Control strategies of atmospheric mercury emissions from coal-fired power plants in China, J. Air Waste Manage. Assoc. 62 (2012) 576–586.
[8] J.F. Ma, C.T. Li, L.K. Zhao, J. Zhang, J.K. Song, G.M. Zeng, X.N. Zhang, Y.E. Xie, Study on removal of elemental mercury from simulated flue gas over activated coke treated by acid, Appl. Surf. Sci. 329 (2015) 292–300.
[9] C.L. Senior, A.F. Sarofim, T.F. Zeng, J.J. Helble, R. Mamani-Paco, Gas-phasse transformations of mercury in coal-fired power plants, Fuel Process. Technol. 63 (2000) 197–213.
[10] C.W. Lee, R.K. Srivastava, S.B. Ghorishi, T.W. Hastings, F.M. Stevens, Investigation of selective catalytic reduction impact on mercury speciation under simulated NOx emission control conditions, J. Air Waste Manage. Assoc. 54 (2004) 1560–1566.
[11] D. Pudasainee, S.J. Lee, S.-H. Lee, J.-H. Kim, H.-N. Jang, S.-J. Cho, Y.-C. Seo, Effect of selective catalytic reactor on oxidation and enhanced removal of mercury in coal-fired power plants, Fuel 89 (2010) 804–809.
[12] P. Forzatti, Present status and perspectives in de-NOx SCR catalysis, Appl. Catal. A: Gen. 222 (2001) 221–236.
[13] R. Zhang, Q. Zhong, W. Zhao, L.M. Yu, H.X. Qu, Promotional effect of fluorine on the selective catalytic reduction of NO with NH_3 over CeO_2–TiO_2 catalyst at low temperature, Appl. Surf. Sci. 289 (2014) 237–244.
[14] W.C. Yu, X.D. Wu, Z.C. Si, D.A. Weng, Influences of impregnation procedure on the SCR activity and alkali resistance of V_2O_5–WO_3/TiO_2 catalyst, Appl. Surf. Sci. 283 (2013) 209–214.
[15] L. Ji, P.M. Sreekanth, P.G. Smirniotis, S.W. Thiel, N.G. Pinto, Manganese oxide/titania materials for removal of NOx and elemental mercury from flue gas, Energy Fuels 22 (2008) 2299–2306.
[16] P.M. Sreekanth, P.G. Smirniotis, Selective reduction of NO with CO over titania supported transition metal oxide catalysts, Catal. Lett. 122 (2007) 37–42.
[17] Y. Li, P. Murphy, C.-Y. Wu, Removal of elemental mercury from simulated coal-combustion flue gas using a SiO_2–TiO_2 nanocomposite, Fuel Process. Technol. 89 (2008) 567–573.
[18] W.Q. Xu, Y.B. Yu, C.B. Zhang, H. He, Selective catalytic reduction of NO by NH_3 over a Ce/TiO_2 catalyst, Catal. Commun. 9 (2008) 1453–1457.
[19] X. Gao, Y. Jiang, Y.C. Fu, Y. Zhong, Z.Y. Luo, K.F. Cen, Preparation and characterization of CeO_2/TiO_2 catalysts for selective catalytic reduction of NO with NH_3, Catal. Commun. 11 (2010) 465–469.
[20] L.A. Chen, J.H. Li, M.F. Ge, R.H. Zhu, Enhanced activity of tungsten modified CeO_2/TiO_2 for selective catalytic reduction of NOx with ammonia, Catal. Today 153 (2010) 77–83.
[21] S.M. Lee, K.H. Park, S.C. Hong, MnOx/CeO_2–TiO_2 mixed oxide catalysts for the selective catalytic reduction of NO with NH_3 at low temperature, Chem. Eng. J. 195–196 (2012) 323–331.
[22] H.L. Li, C.-Y. Wu, Y. Li, J.Y. Zhang, Superior activity of MnOx–CeO_2/TiO_2 catalyst for catalytic oxidation of elemental mercury at low flue gas temperatures, Appl. Catal. B: Environ. 111 (2012) 381–388.
[23] L. Chen, J.H. Li, M.F. Ge, Promotional effect of Ce-doped V_2O_5–WO_3/TiO_2 with low vanadium loadings for selective catalytic reduction of NOx by NH_3, J. Phys. Chem. C 113 (2009) 21177–21184.
[24] G. Qi, R.T. Yang, Performance and kinetics study for low-temperature SCR of NO with NH_3 over MnOx–CeO_2 catalyst, J. Catal. 217 (2003) 434–441.
[25] L.H. Tian, C.T. Li, Q. Li, G.M. Zeng, Z. Gao, S.H. Li, X.P. Fan, Removal of elemental mercury by activated carbon impregnated with CeO_2, Fuel 88 (2009) 1687–1691.
[26] X.P. Fan, C.T. Li, G.M. Zeng, Z. Gao, L. Chen, W. Zhang, H.L. Gao, Removal of gas-phase element mercury by activated carbon fiber impregnated with CeO_2, Energy Fuels 24 (2010) 4250–4254.
[27] S.S. Tao, C.T. Li, X.P. Fan, G.M. Zeng, P. Lu, X. Zhang, Q.B. Wen, W.W. Zhao, D.Q. Luo, C.Z. Fan, Activated coke impregnated with cerium chloride used for elemental mercury removal from simulated flue gas, Chem. Eng. J. 210 (2012) 547–556.
[28] X.Y. Wen, C.T. Li, X.P. Fan, H. Gao, W. Zhang, L. Chen, G. Zeng, Y. Zhao, Experimental study of gaseous elemental mercury removal with CeO_2/γ-Al_2O_3, Energy Fuels 25 (2011) 2939–2944.
[29] X.P. Fan, C.T. Li, G.M. Zeng, X. Zhang, S.S. Tao, P. Lu, Y. Tan, D.Q. Luo, Hg^0 removal from simulated flue gas over CeO_2/HZSM-5, Energy Fuels 26 (2012) 2082–2089.
[30] H.L. Li, C.Y. Wu, Y. Li, J.Y. Zhang, CeO_2–TiO_2 catalysts for catalytic oxidation of elemental mercury in low-rank coal combustion flue gas, Environ. Sci. Technol. 45 (2011) 7394–7400.
[31] J. He, G.K. Reddy, S.W. Thiel, P.G. Smirniotis, N.G. Pinto, Ceria-modified manganese oxide/titania materials for removal of elemental and oxidized mercury from flue gas, J. Phys. Chem. C 115 (2011) 24300–24309.
[32] Z.M. Liu, S.X. Zhang, J.H. Li, J.Z. Zhu, L.L. Ma, Novel V_2O_5–CeO_2/TiO_2 catalyst with low vanadium loading for the selective catalytic reduction of NOx by NH_3, Appl. Catal. B: Environ. 158–159 (2014) 11–19.
[33] Y.S. Shen, D.H. Zheng, B. Yang, S.B. Ni, S.M. Zhu, Synergetic catalysis of ceria and titania for selective reduction of NO, J. Rare Earth 30 (2012) 431–436.
[34] J. Fang, F.C. Shi, H.Z. Bao, K. Qian, Z.Q. Jiang, W.X. Huang, Evolution of surface and bulk structures of Ce*x*Ti1–*x*O_2 oxide composites, Chin. J. Catal. 34 (2013) 2075–2083.
[35] C. Richardson, T. Machalek, S. Miller, C. Dene, R. Chang, Effect of NOx control processes on mercury speciation in utility flue gas, J. Air Waste Manage. Assoc. 52 (2002) 941–947.
[36] Y. Eom, S.H. Jeon, T.A. Ngo, J. Kim, T.G. Lee, Heterogeneous mercury reaction on a selective catalytic reduction (SCR) catalyst, Catal. Lett. 121 (2007) 219–225.
[37] H.L. Li, C.Y. Wu, Y. Li, L.Q. Li, Y.C. Zhao, J.Y. Zhang, Role of flue gas components in mercury oxidation over TiO_2 supported MnOx–CeO_2 mixed-oxide at low temperature, J. Hazard. Mater. 243 (2012) 117–123.
[38] A.A. Presto, E.J. Granite, Survey of catalysts for oxidation of mercury in flue gas, Environ. Sci. Technol. 40 (2006) 5601–5609.
[39] S.H. Qiao, J. Chen, J.F. Li, Z. Qu, P. Liu, N.Q. Yan, J.Q. Jia, Adsorption and catalytic oxidation of gaseous elemental mercury in flue gas over MnOx/alumina, Ind. Eng. Chem. Res. 48 (2009) 3317–3322.
[40] N.Q. Yan, W.M. Chen, J. Chen, Z. Qu, Y.F. Guo, S.J. Yang, J.P. Jia, Significance of RuO_2 modified SCR catalyst for elemental mercury oxidation in coal-fired flue gas, Environ. Sci. Technol. 45 (2011) 5725–5730.
[41] J. Fang, H.Z. Bao, B. He, F. Wang, D.J. Si, Z.Q. Jiang, Z.Y. Pan, S.Q. Wei, W.X. Huang, Interfacial and surface structures of CeO_2–TiO_2 mixed oxides, J. Phys. Chem. C 111 (2007) 19078–19085.
[42] Y. Huang, Z.Q. Tong, B. Wu, J.F. Zhang, Low temperature selective catalytic reduction of NO by ammonia over V_2O_5–CeO_2/TiO_2, J. Fuel. Chem. Technol. 36 (2008) 616–620.
[43] Z.B. Wu, R.B. Jin, Y. Liu, H.Q. Wang, Ceria modified MnOx/TiO_2 as a superior catalyst for NO reduction with NH_3 at low-temperature, Catal. Commun. 9 (2008) 2217–2220.
[44] J. Yang, Q. Yang, J. Sun, Q.C. Liu, D. Zhao, W. Gao, L. Liu, Effects of mercury oxidation on V_2O_5–WO_3/TiO_2 catalyst properties in NH_3-SCR process, Catal. Commun. 59 (2015) 78–82.
[45] L. Qu, C.T. Li, G.M. Zeng, M.Y. Zhang, M.F. Fu, J.F. Ma, F.M. Zhan, D.Q. Luo, Support modification for improving the performance of MnOx–CeOy/γ-Al_2O_3 in selective catalytic reduction of NO by NH_3, Chem. Eng. J. 242 (2014) 76–85.
[46] J. Fang, X.Z. Bi, D.J. Si, Z.Q. Jiang, W.X. Huang, Spectroscopic studies of interfacial structures of CeO_2–TiO_2 mixed oxides, Appl. Surf. Sci. 253 (2007) 8952–8961.
[47] X.P. Fan, C.T. Li, G.M. Zeng, X. Zhang, S.S. Tao, P. Lu, S.H. Li, Y.P. Zhao, The effects of Cu/HZSM-5 on combined removal of Hg^0 and NO from flue gas, Fuel Process. Technol. 104 (2012) 325–331.
[48] Y.S. Gao, Z. Zhang, J.W. Wu, L.H. Duan, A. Umar, L. Sun, Z.H. Guo, Q. Wang, A critical review on the heterogeneous catalytic oxidation of elemental mercury in flue gases, Environ. Sci. Technol. 47 (2013) 10813–10823.
[49] E.J. Granite, H.W. Pennline, R.A. Hargis, Novel sorbents for mercury removal from flue gas, Ind. Eng. Chem. Res. 39 (2000) 1020–1029.